

Improved measurements of neutron lifetime with cold neutron beam at J-PARC

Y. Fuwa,^{1,2} T. Hasegawa,³ K. Hirota,⁴ T. Hoshino,⁵ R. Hosokawa,⁶ G. Ichikawa,^{4,2} S. Ieki,⁷ T. Ino,^{4,2} Y. Iwashita,⁸ M. Kitaguchi,^{3,9} R. Kitahara,^{10,11} S. Makise,⁵ K. Mishima,^{9,4,*} T. Mogi,⁷ N. Nagakura,⁷ H. Oide,⁴ H. Okabe,³ H. Otono,¹² Y. Seki,¹³ D. Sekiba,¹⁴ T. Shima,¹⁵ H. E. Shimizu,¹⁶ H. M. Shimizu,³ N. Sumi,⁴ H. Sumino,¹⁷ M. Tanida,⁵ H. Uehara,⁵ T. Yamada,⁷ S. Yamashita,¹⁸ K. Yano,⁵ and T. Yoshioka¹⁹

¹Japan Atomic Energy Agency, Tokai 319-1195, Japan

²J-PARC Center, Tokai 319-1195, Japan

³Department of Physics, Graduate School of Science, Nagoya University, Nagoya 464-8602, Japan

⁴High Energy Accelerator Research Organization, Tsukuba 305-0801, Japan

⁵Department of Physics, Graduate School of Science, Kyushu University, Fukuoka 819-0395, Japan

⁶Faculty of Science and Engineering, Iwate University, Morioka 020-8551, Japan

⁷Department of Physics, Graduate School of Science,
The University of Tokyo, Tokyo 113-0033, Japan

⁸Institute for Integrated Radiation and Nuclear Science, Kyoto University, Osaka 590-0494, Japan

⁹Kobayashi-Maskawa Institute, Nagoya University, Nagoya 464-8602, Japan

¹⁰Department of Physics, Kyoto University, Kyoto, 606-8502, Japan

¹¹Technology Research Center, Sumitomo Heavy Industries, Ltd., Yokosuka, 237-8555, Japan

¹²Department of Physics, Faculty of Sciences, Kyushu University, Fukuoka 819-0395, Japan

¹³Institute of Multidisciplinary Research for Advanced Materials, Tohoku University, Sendai 980-8577, Japan

¹⁴Institute of Applied Physics, University of Tsukuba, Tsukuba 305-8573, Japan

¹⁵Research Center for Nuclear Physics, Osaka University, Ibaraki 567-0047, Japan

¹⁶SOKENDAI, Shonan Village, Hayama 240-0193, Japan

¹⁷Research Center for Advanced Science and Technology,
The University of Tokyo, Tokyo 153-0041, Japan

¹⁸Research and Regional Cooperation Office, Iwate Prefectural University, Takizawa 020-0693, Japan

¹⁹Research Center for Advanced Particle Physics, Kyushu University, Fukuoka 819-0395, Japan

(Dated: December 30, 2024)

The “neutron lifetime puzzle” arises from the discrepancy between neutron lifetime measurements obtained using the beam method, which measures decay products, and the bottle method, which measures the disappearance of neutrons. To resolve this puzzle, we conducted an experiment using a pulsed cold neutron beam at J-PARC. In this experiment, the neutron lifetime is determined from the ratio of neutron decay counts to ${}^3\text{He}(n,p){}^3\text{H}$ reactions in a gas detector. This experiment belongs to the beam method but differs from previous experiments that measured protons, as it instead detects electrons, enabling measurements with distinct systematic uncertainties. By enlarging the beam transport system and reducing systematic uncertainties, we achieved a fivefold improvement in precision. Analysis of all acquired data yielded a neutron lifetime of $\tau_n = 877.2 \pm 1.7_{(\text{stat.})}^{+4.0}_{-3.6(\text{sys.})}$ s. This result is consistent with bottle method measurements but exhibits a 2.3σ tension with the average value obtained from the proton-detection-based beam method.

Introduction— A neutron decays into three particles, a proton, an electron, and an antineutrino via weak interactions. The neutron β decay lifetime, τ_n , is a crucial parameter that determines the neutron-to-proton ratio at the onset of Big Bang nucleosynthesis (BBN) [1, 2]. The combination of the BBN model and the baryon-to-photon ratio derived from the cosmic microwave background observations [3, 4] provides an accurate prediction of the abundance of light elements, allowing tests of physical phenomena in the early universe. Additionally, the V_{ud} term in the Cabibbo-Kobayashi-Maskawa (CKM) matrix can be determined using τ_n and λ , which is the ratio of axial-vector to vector coupling constants, g_A/g_V , independently of nuclear models. Revised radiative corrections in 2018 [5] suggested the CKM unitarity violation exceeding 2σ [6], emphasizing the importance of the measurement of the neutron lifetime. Precise data on τ_n is also valuable for testing lattice QCD calculations

of g_A [7].

Neutron lifetime has been measured using two primary methods. The first is the beam method [8, 9], where neutron β decay products, specifically protons in these references, are counted relative to the number of incident neutrons, yielding an average lifetime of $\tau_n^{\text{beam}} = 888.0 \pm 2.0$ s. The second is the bottle method [10–17], which measures the disappearance of ultra-cold neutrons (UCNs) confined in a container over time, producing an average value of $\tau_n^{\text{bottle}} = 878.4 \pm 0.5$ s. The 9.5-s (4.6σ) discrepancy between the two methods is known as the “neutron lifetime puzzle” [18], raising concerns about the reliability of neutron lifetime measurements.

Possible causes for this discrepancy include unaccounted systematic uncertainties, such as protons from neutron decay undergoing charge exchange with residual gas [19], though this effect is considered negligible [20]. The 9.5-s, approximately 1% discrepancy between beam

and bottle methods has caused discussions of theories such as UCN inelastic scattering with dark matter [21], hydrogen atom formation [22], mirror neutron transitions [23], or neutron decay into dark matter [24]. Upcoming experiments [25–28], including space neutron detections [29, 30], may help resolve this issue.

To address the neutron lifetime puzzle, we conducted neutron lifetime measurements using the high-intensity pulsed neutron beamline at Japan Proton Accelerator Research Complex (J-PARC), adopting the method of Kossakowski et al. [31]. This experiment detects electrons from neutron β decay, offering a distinct observable compared to previous proton-counting beam methods [8, 9], and thus provides an alternative approach to verify the neutron lifetime puzzle. Our first result in 2020, $\tau_n = 898 \pm 10_{(\text{stat.})}^{+15}_{-18(\text{sys.})}$ s [32], was consistent with both beam and bottle methods. Through improved neutron intensity by a new neutron transport and reduced systematic uncertainties, we achieved a fivefold improvement in precision, as discussed in this paper.

Principle of the experiment– The experiment, conducted at the polarized neutron beam branch of BL05/NOP at J-PARC Materials and Life Science Experimental Facility [33, 34], is illustrated schematically in Fig. 1. The pulsed neutron beam is shaped into 40-cm-long bunches using a spin flip chopper (SFC) [35–37] and introduced into a 1-m-long time projection chamber (TPC) [38]. Measuring β decay events while the neutron bunch is fully within the TPC reduces uncertainties in detection efficiency and effects from the background.

The TPC is filled with an He+CO₂ gas with a mixture of 85:15, optimized for low neutron scattering and efficient electron multiplication. This setup achieves a trigger efficiency of over 99.9% for neutron β decay events. A precise amount of ³He, corresponds to the pressure of 50 mPa, is added using a volumetric expansion method, and ³He(n,p)³H reactions are used to determine the number of incident neutrons. The inner walls of the beam duct and TPC are covered with a shielding material made of a mixture of ⁶Li-enriched LiF and polytetrafluoroethylene (PTFE) in a 30:70 weight ratio [39]. This cover effectively reduces background γ radiation produced by neutron capture.

The neutron lifetime is derived using the detected β decay count S_β , the ³He(n,p)³H reaction count S_{He} , their respective detection efficiencies ε_β and ε_{He} , the number density of ³He in the detector ρ , and the ³He(n,p)³H reaction cross-section σ_0 at the neutron velocity $v_0 = 2200$ m/s, according to the following equation [32]:

$$\tau_n = \frac{1}{\rho\sigma_0 v_0} \left(\frac{S_{\text{He}}/\varepsilon_{\text{He}}}{S_\beta/\varepsilon_\beta} \right). \quad (1)$$

The β decay events and ³He(n,p)³H events are identified using waveform and track information from the TPC.

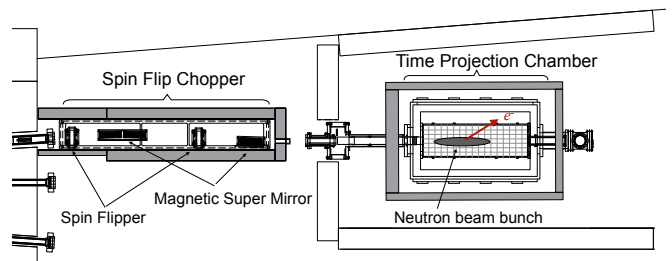


FIG. 1. The top view of BL05/NOP. Pulsed neutrons entering from the beam port on the left are shaped into bunches by the spin flip chopper and then directed into the time projection chamber.

The neutron lifetime is calculated from their count ratio and detection efficiencies, determined by using Monte Carlo simulations (MCs) based on Geant4.9.6 [40].

Updates– We conducted experiments with improvements to the apparatus and analysis based on the 2020 results [32]. A major source of systematic uncertainties was background γ rays from the absorption reactions of neutrons scattered by the TPC working gas. To address this, we reduced the gas pressure to mitigate neutron scattering and its associated effects. Lower pressures made the TPC more prone to electrical discharge, necessitating reduced signal amplification. By minimizing electrical noise and optimizing the operating conditions, we successfully obtained stable measurements at 50 kPa, reduced from the original pressure of 100 kPa. In addition, simulations were developed to reproduce these low-pressure conditions, incorporating specific wire efficiency and space charge. These simulations thereby enable reliable measurements at 50 kPa. The low-pressure measurements further improved the accuracy of determining the ³He content in the working gas and also reduced background events caused by nuclear reactions with CO₂, namely ¹²C(n, γ)¹³C and ¹⁷O(n, α)¹⁴C.

The TPC operating gas used is commercially available high-grade He gas (G1He) containing 0.1 ppm of ³He [32]. Previously, the amount of ³He was determined by analyzing G1He using a mass spectrometer [41, 42]. After measuring the ¹⁴N(n,p)¹⁴C reaction cross section with a precision of 0.4% [43], we established a method to determine the ³He/⁴He ratio in G1He with an accuracy of better than 0.8% by performing measurements with He+CO₂ gas mixed with N₂ gas [44]. We also improved the method for determining the amount of ³He introduced into the TPC vacuum vessel. In this experiment, 50 mPa of ³He gas is precisely injected using a buffer vessel with a known volume ratio to the vacuum chamber. By employing two pressure gauges with different dynamic ranges and an optimized buffer volume, the measurement precision of the volume ratio improved from 0.34% to 0.12%. Consequently, the accuracy of ρ determination at 50 kPa was enhanced to 0.13% [44].

These methods have been adopted since 2019.

We use an SFC to bunch neutrons incident to the TPC. The neutron intensity was previously limited by the size of the neutron mirrors of the SFC [35]. The upgraded SFC, featuring larger magnetic supermirrors and spin flippers, increased the neutron intensity to the TPC by a factor of 2.8 while maintaining a signal-to-noise ratio of 250–400 [35–37]. Measurements were performed under four conditions: two gas pressures (100 kPa and 50 kPa) and two SFC configurations (old and new SFC). Table I summarizes the dataset, comprising 49 gas fills measured between 2014 and 2023. Each gas fill represents a measurement of approximately one week, including energy calibration with a ^{55}Fe source, drift time calibration using cosmic rays, neutron lifetime measurements with beam passage, and background measurements with a beam shutter closed. During the measurement, the beam alternated periodically between a beam pass run (1000–1200 s) and a beam dump run (800–1000 s).

TABLE I. Measurements for each condition, presented as the number of gas fills and beam cycles (defined as one beam pass run and one dump run).

Conditions	Year	Gas fill	Beam cycle
100 kPa/old SFC	2014–2019	29	4660
50 kPa/old SFC	2017–2018	6	1044
100 kPa/new SFC	2021–2023	5	671
50 kPa/new SFC	2021–2023	9	1729

Analysis– The analysis follows the method of previous measurements [32]. Two parameters, X_E and X_C are introduced to separate β decay events from the background. Here, X_E is the distance between the near endpoint of a track and the central wire, while X_C indicates the distance from the closest hit to the center, expressed in wire spacing units (Fig.2). Since neutron β decay events originate from the beam region (40 mm), the signal region was defined as $X_E < 5$ (< 60 mm). On the other hand, the region $X_C \geq 5$ contains almost no events originating from neutron β decay and was therefore defined as the background region.

The primary background in this experiment arises from (n, γ) events caused by neutrons scattered by the TPC working gas. The number of background events to be subtracted can be obtained by multiplying the number of events in the background region by the ratio of those entering the signal region to those in the background region. This ratio is determined using MCs. A larger background than predicted by MC simulations was observed, amounting to 4.9–5.4% of S_β at 100 kPa (vs. 1.2–1.3% predicted) and 3.1–3.3% at 50 kPa (vs. 0.65–0.67%). While the cause remains unclear, leakage of scattered neutrons through gaps in the ^6LiF tile is suspected. To model this background, we selected MCs assuming discrete γ ray energies that best reproduced the experimental results. Since the single-energy distribution used in the previous

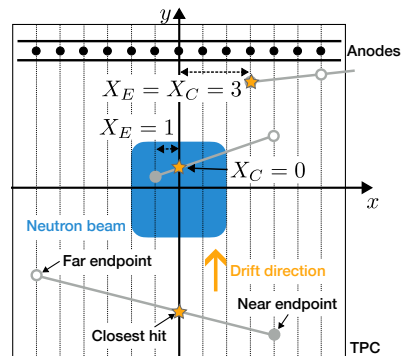


FIG. 2. Conceptual downstream view of the TPC illustrating X_E (distance from the near endpoint of a track to central wire) and X_C (distance from closest hit to center). Number of wires and beam size are not to scale.

method [32] could not reproduce the background shape or the energy loss per unit length (dE/dx) distribution, we constructed MCs with γ rays with two energy components. The γ ray energies were determined to reproduce the two-dimensional distribution of X_E and X_C outside the signal region. The origins of the γ rays were considered: “Internal,” for neutron absorption within the ^6LiF tile shielding, and “Internal-external,” for absorption within and outside the shielding. The “Internal-external” model, with 200 keV contributing 91.9(8)% and 5000 keV contributing 8.1(8)%, showed the best fit to the experimental data with the χ^2 per degrees of freedom (DOF) of 208.8/202.

Signal cut uncertainties were evaluated by varying the X_E cut from 4 ch to 11 ch (5 ch as baseline), with a maximum variation of 0.2% in the data-to-MC event ratio (Fig. 3). Energy cut uncertainties, estimated from dE/dx differences for cosmic rays, contributed less than 0.1%. These improvements ensured accurate background subtraction and enhanced the reliability of neutron β decay measurements.

The W-value, the average energy required for single-electron ionization, in the He+CO₂ gas of a proton (W_p) increases as proton energy decreases below 1 keV unlike electron ionization (W_e) [45]. We previously addressed the effect by simplifying the quenching factor as $q(E) = W_e(E)/W_p(E) = 1$ with kinetic energy E , while accounting for the impact of $q(E) = 0$ as a 0.6% systematic uncertainty. Improved statistics now make this effect significant, thus $q(E)$ value from SRIM [46], ranging from 0.2 to 0.6 for 25–750 eV protons, were adopted. This adjustment reduced MC detection efficiency ε_β by up to 0.3%, with a systematic uncertainty of 0.1% based on differences between W-values from SRIM and at which MCs give best fits.

Pileup events were estimated based on count rates. The full pileup rate corresponds to a lifetime change of 0.4%. We evaluated the classification of primary pileup

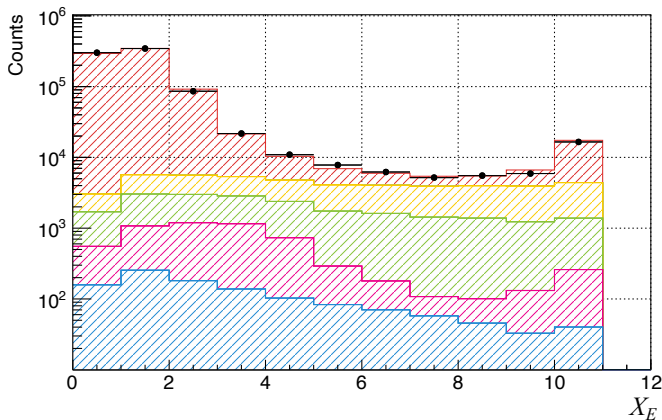


FIG. 3. X_E distribution for 50 kPa/new SFC. Black points represent measured data, and colored regions represent the stacked MC distributions. From top to bottom: red (β), yellow (gas-scattered 5000 keV γ rays), green (gas-scattered 200 keV γ rays), magenta (γ rays scattered by the ${}^6\text{LiF}$ tile shutter), and blue (β events from gas-scattered neutrons).

events, triggered by a β decay electron and a ${}^3\text{He}$ event follows, by developing a dedicated MC simulation that generates events at different timings. This improved the classification accuracy, reducing the pileup uncertainty to $+0.17/-0.07\%$.

Results– To mitigate human bias, a random variation of $\pm 10\%$ has been applied to ρ during the updated analysis, which was removed only after the analysis method and parameters had been finalized. Data were grouped into four conditions based on gas pressure (100 kPa and 50 kPa) and SFC type (old and new), with average neutron lifetimes summarized in Table II. For each condition, uncertainties related to cut positions were evaluated independently, while globally correlated uncertainties were applied as common shifts. The overall neutron lifetime result from J-PARC, combining all conditions, is $\tau_n = 877.2 \pm 1.7_{(\text{stat.})} \pm 4.0_{-3.6}^+(\text{sys.})$. The combining average yielded $\chi^2/\text{DOF} = 15.8/3$, though the underlying cause of this deviation remains undetermined.

TABLE II. Neutron lifetime values for each gas pressure (100 kPa, 50 kPa) and SFC configuration (new, old), with averages. Units in seconds.

Conditions	Value	Stat.	Cut position	Other sys.
100 kPa/old SFC	870.9	3.5	+1.8/-2.8	+5.5/-4.9
100 kPa/new SFC	868.3	4.0	+1.5/-2.9	+3.8/-3.2
50 kPa/old SFC	868.2	7.7	+2.7/-0.9	+4.8/-3.9
50 kPa/new SFC	884.8	2.4	+0.8/-1.3	+3.2/-3.0
Combined	877.2	1.7		+4.0/-3.6

The main uncertainties in this measurement are summarized in Table III, with the largest contribution from the gas-scattering neutron background. The effect due to the cut position uncertainties are small (0.9 s) due to good agreement between MC simulations and exper-

TABLE III. List of uncertainties with units in seconds.

Effect	Uncertainty
Statistic	1.7
Cut position	0.9
Gas-induced background	+1.1/-2.0
Pile up	+1.5/-0.6
Contamination from ${}^{12}\text{C}(n,\gamma){}^{13}\text{C}$	+1.7/-0.0
γ -ray scattering at LiF shutter	1.3
Unbunched neutron from SFC	+1.1/-1.0
Inject ${}^3\text{He}$	1.2
${}^3\text{He}$ in G1He	+1.5/-1.4
${}^3\text{He}(n,p){}^3\text{H}$ cross section	1.2
Total systematic	+4.0/-3.6

imental results. The ${}^{12}\text{C}(n,\gamma){}^{13}\text{C}$ reaction, where ${}^{12}\text{C}$ in the CO_2 gas absorbs neutrons, produces ${}^{13}\text{C}$ with a 4946 keV γ ray and a 1.0 keV recoil. Misclassification of these events as β decay was evaluated using MC simulations, with uncertainties near the energy threshold included in the systematic uncertainty. The effect due to scattering of γ rays at the ${}^6\text{LiF}$ tile shutter was modeled using PHITS3.20 [47] and NaI detector measurements. This contributed to a 1.3 s systematic uncertainty. The effect of unbunched neutrons caused by SFC imperfections, leading to detection efficiency mismatches for β and ${}^3\text{He}(n,p){}^3\text{H}$ events at the TPC edges, was simulated to evaluate their impact and incorporated as systematic uncertainties. The uncertainties in introduced ${}^3\text{He}$ and G1He-contained ${}^3\text{He}$ were incorporated into ρ . For 50 kPa operations, ${}^{14}\text{N}$ -based measurements limited the uncertainty to 0.5 s, while mass spectrometer data increased it to 1.5 s. The ${}^3\text{He}(n,p){}^3\text{H}$ cross-section, 5333 ± 7 barn [48] obtained by averaging two experiments [49, 50], contributed 1.2 s of uncertainty.

The neutron lifetime obtained in this study, with statistical and systematic uncertainties combined in quadrature is shown in Fig.4, along with results from previous experiments [6]. Our value is consistent with the bottle method but shows a 2.3σ tension with the average of the proton-counting beam method. Combining our results with other beam measurements gives $\tau_n^{\text{beam}} = 886.0 \pm 1.8$, reducing the discrepancy with the bottle method to 4.0σ .

Conclusion and outlook– To address the “neutron lifetime puzzle,” arising from discrepancies between neutron lifetimes measured by the beam method (via decay products) and the bottle method (via disappearance), we measured the neutron lifetime from the ratio of electrons from neutron decay to ${}^3\text{He}(n,p){}^3\text{H}$ reactions. Unlike previous beam method experiments that detected protons, this experiment introduced distinct systematic uncertainties.

By enlarging the SFC aperture, the neutron intensity increased by a factor of 2.8, enabling high-statistics data acquisition and achieving a statistical precision of 1.7 s. Systematic uncertainties were reduced to 4 s by

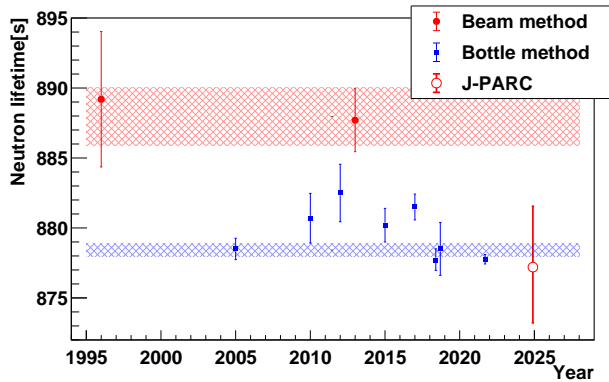


FIG. 4. Measured neutron lifetimes in this work and previous experiments [6]. Red circles represent measurements using the proton-detection-based beam method, blue squares represent the bottle method, and the red and blue bands indicate the averages of these two methods. The open circle represents the measurement from this work at J-PARC.

accurately modeling gas-scattered neutron backgrounds. Combining all data, the neutron lifetime was determined as $\tau_n = 877.2 \pm 1.7_{(\text{stat.})}^{+4.0} - 3.6_{(\text{sys.})}$ s. This result aligns with the bottle method and is 10.8 s shorter than the averaged value of proton-counting beam method, exhibiting 2.3σ tension in the results of the beam method.

The primary limitation of this experiment is the γ ray background from gas-scattered neutrons in the TPC. To suppress this background, the upcoming LiNA experiment [51, 52] will apply a solenoidal magnetic field to the TPC. This setup is expected to reduce background events by a factor of 50. Furthermore, the reduction of background will decrease the required measurement time to one-third, while the uncertainty due to pileup is also anticipated to decrease to one-third as a result of its shorter drift length.

We sincerely thank Prof. Y. Namito and H. Hirayama for the discussions on Geant4 specifications, and Prof. M. Hino for fabricating the neutron supermirror for the SFC. This work was supported by JSPS KAKENHI Grant Numbers (JP19GS0210, 23244047, 24654058, 26247035, 16H02194, 18H01231, 19H00690, 21H04475, and 22H00140), and JST, the establishment of university fellowships towards the creation of science technology innovation, Grant Number JPMJFS2136. The neutron experiment at the Materials and Life Science Experimental Facility of J-PARC was performed under user programs (Proposal Nos. 2014B0271, 2015A0316, 2016A0168, 2016B0272, 2017A0230, 2017B0332, 2018A0297, 2018B0272, 2019A0223, 2019B0341, 2020A0223, 2021B0287, 2022A0117, 2022B0325, 2023A0184, 2023B0253, and 2024A0331) and an S-type projects of KEK IMSS (Proposal Nos. 2014S03 and 2019S03). This experiment is supported as stage-1 status (E100) of J-PARC-PAC

KEK IPNS.

- * Corresponding author: kmishima@kmi.nagoya-u.ac.jp
- [1] G. J. Mathews, T. Kajino, and T. Shima, Big bang nucleosynthesis with a new neutron lifetime, *Phys. Rev. D* **71**, 021302 (2005).
 - [2] T. Chowdhury and S. Ipek, Neutron lifetime anomaly and Big Bang nucleosynthesis, *Can. J. Phys.* **102**, 96 (2024).
 - [3] C. L. Bennett, D. Larson, J. L. Weiland, N. Jarosik, G. Hinshaw, N. Odegard, K. Smith, R. Hill, B. Gold, M. Halpern, *et al.*, Nine-year Wilkinson Microwave Anisotropy Probe (WMAP) observations: final maps and results, *Astrophys. J., Suppl. Ser.* **208**, 20 (2013).
 - [4] N. Aghanim, Y. Akrami, F. Arroja, M. Ashdown, J. Aumont, C. Baccigalupi, M. Ballardini, A. J. Banday, R. Barreiro, N. Bartolo, *et al.*, Planck 2018 results-I. Overview and the cosmological legacy of Planck, *Astron. Astrophys.* **641**, A1 (2020).
 - [5] C.-Y. Seng, M. Gorchtein, H. H. Patel, and M. J. Ramsey-Musolf, Reduced Hadronic Uncertainty in the Determination of V_{ud} , *Phys. Rev. Lett.* **121**, 241804 (2018).
 - [6] S. Navas *et al.* (Particle Data Group Collaboration), Review of Particle Physics, *Phys. Rev. D* **110**, 030001 (2024).
 - [7] C.-C. Chang, A. N. Nicholson, E. Rinaldi, E. Berkowitz, N. Garron, D. A. Brantley, H. Monge-Camacho, C. J. Monahan, C. Bouchard, M. A. Clark, *et al.*, A per-cent-level determination of the nucleon axial coupling from quantum chromodynamics, *Nature* **558**, 91 (2018).
 - [8] J. Byrne, P. Dawber, C. G. Habeck, S. J. Smidt, J. Spain, and A. P. Williams, A revised value for the neutron lifetime measured using a Penning trap, *Europhys. Lett.* **33**, 187 (1996).
 - [9] A. T. Yue, M. S. Dewey, D. M. Gilliam, G. L. Greene, A. B. Laptev, J. S. Nico, W. M. Snow, and F. E. Wietfeldt, Improved Determination of the Neutron Lifetime, *Phys. Rev. Lett.* **111**, 222501 (2013).
 - [10] A. Serebrov, V. Varlamov, A. Kharitonov, A. Fomin, Y. Pokotilovski, P. Geltenbort, J. Butterworth, I. Krasnoschekova, M. Lasakov, R. Tal'Daev, A. Vassiljev, and O. Zherebtsov, Measurement of the neutron lifetime using a gravitational trap and a low-temperature Fomblin coating, *Phys. Lett. B* **605**, 72 (2005).
 - [11] A. Pichlmaier, V. Varlamov, K. Schreckenbach, and P. Geltenbort, Neutron lifetime measurement with the UCN trap-in-trap MAMBO II, *Phys. Lett. B* **693**, 221 (2010).
 - [12] A. Steyerl, J. Pendlebury, C. Kaufman, S. S. Malik, and A. Desai, Quasielastic scattering in the interaction of ultracold neutrons with a liquid wall and application in a reanalysis of the Mambo I neutron-lifetime experiment, *Phys. Rev. C: Nucl. Phys.* **85**, 065503 (2012).
 - [13] S. Arzumanov, L. Bondarenko, S. Chernyavsky, P. Geltenbort, V. Morozov, V. Nesvizhevsky, Y. Panin, and A. Strepetov, A measurement of the neutron lifetime using the method of storage of ultracold neutrons and detection of inelastically up-scattered neutrons, *Phys. Lett. B* **745**, 79 (2015).
 - [14] A. P. Serebrov, E. A. Kolomensky, A. K. Fomin, I. A.

- Krasnoshchekova, A. V. Vassiljev, D. M. Prudnikov, I. V. Shoka, A. V. Chechkin, M. E. Chaikovskiy, V. E. Varlamov, *et al.*, Neutron lifetime measurements with a large gravitational trap for ultracold neutrons, *Phys. Rev. C* **97**, 055503 (2018).
- [15] R. W. Pattie, N. B. Callahan, C. Cude-Woods, E. R. Adamek, L. J. Broussard, S. M. Clayton, S. A. Currie, E. B. Dees, X. Ding, E. M. Engel, *et al.*, Measurement of the neutron lifetime using a magneto-gravitational trap and in situ detection, *Science* **360**, 627 (2018).
- [16] V. F. Ezhov, A. Andreev, G. Ban, B. Bazarov, P. Geltenbort, A. Glushkov, V. Knyazkov, N. A. Kovrizhnykh, G. Krygin, O. Naviliat-Cuncic, *et al.*, Measurement of the neutron lifetime with ultracold neutrons stored in a magneto-gravitational trap, *JETP Lett.* **107**, 671 (2018).
- [17] F. M. Gonzalez, E. Fries, C. Cude-Woods, T. Bailey, M. Blatnik, L. Broussard, N. Callahan, J. Choi, S. Clayton, S. Currie, *et al.* (UCN τ Collaboration), Improved neutron lifetime measurement with UCN τ , *Phys. Rev. Lett.* **127**, 162501 (2021).
- [18] G. Greene and P. Geltenbort, A puzzle lies at the heart of the atom, *Sci. Am.* **314**, 36 (2016).
- [19] A. Serebrov, M. Chaikovskii, G. Klyushnikov, O. Zhrebtsov, and A. Chechkin, Search for explanation of the neutron lifetime anomaly, *Phys. Rev. D* **103**, 074010 (2021).
- [20] F. E. Wietfeldt, R. Biswas, J. Caylor, B. Crawford, M. S. Dewey, N. Fomin, G. L. Greene, C. C. Haddock, S. F. Hoogerheide, H. P. Mumm, *et al.*, Comment on “Search for explanation of the neutron lifetime anomaly”, *Phys. Rev. D* **107**, 118501 (2023).
- [21] S. Rajendran and H. Ramani, Composite solution to the neutron lifetime anomaly, *Phys. Rev. D* **103**, 035014 (2021).
- [22] E. Oks, New results on the two-body decay of neutrons shed new light on neutron stars, *New Astron.* **113**, 102275 (2024).
- [23] Z. Berezhiani, Neutron lifetime puzzle and neutron-mirror neutron oscillation, *Eur. Phys. J. C* **79**, 1 (2019).
- [24] B. Fornal and B. Grinstein, Dark matter interpretation of the neutron decay anomaly, *Phys. Rev. Lett.* **120**, 191801 (2018).
- [25] S. Materne, R. Picker, I. Altarev, H. Angerer, B. Franke, E. Gutmiedl, F. Hartmann, A. Müller, S. Paul, and R. Stoeppler, PENeLOPE—on the way towards a new neutron lifetime experiment with magnetic storage of ultra-cold neutrons and proton extraction, *Nucl. Instrum. Methods Phys. Res., Sect. A* **611**, 176 (2009).
- [26] W. Wei, A new neutron lifetime experiment with cold neutron beam decay in superfluid helium-4, *J. Phys. G:Nucl. Part. Phys.* **47**, 125101 (2020).
- [27] J. Auler, M. Engler, K. Franz, J. Kahlenberg, J. Karch, N. Pfeifer, K. Roß, C. Strid, N. Yazdandoost, E. Adamek, *et al.*, τ SPECT: a spin-flip loaded magnetic ultracold neutron trap for a determination of the neutron lifetime, *J. Phys. G:Nucl. Part. Phys.* **51**, 115103 (2024).
- [28] M. Krivoš, N. Floyd, Z. Tang, C. Morris, M. Blatnik, S. Clayton, C. Cude-Woods, A. Holley, D. Hooks, T. Ito, *et al.*, Cerium doped yttrium aluminum perovskite scintillator as an absolute ultracold neutron detector, *Review of Scientific Instruments* **95**, 10.1063/5.0211059 (2024).
- [29] J. T. Wilson, D. J. Lawrence, P. N. Peplowski, V. R. Eke, and J. A. Kegerreis, Measurement of the free neutron lifetime using the neutron spectrometer on NASA’s Lunar Prospector mission, *Phys. Rev. C* **104**, 045501 (2021).
- [30] N. Tsuji, T. Enoto, H. Nagaoka, Y. Kato, K. Taniguchi, M. Hareyama, Y. Otake, Y. Wakabayashi, T. Takanashi, C. Iwamoto, *et al.*, Moon Moisture Targeting Observatory (MoMoTarO) for basic science application to neutron lifetime measurement, in *Proceedings of 38th International Cosmic Ray Conference (ICRC2023) - Cosmic-Ray Physics (Indirect, CRI)*, Vol. 444 (2023) p. 296.
- [31] R. Kossakowski, P. Grivot, P. Liaud, K. Schreckenbach, and G. Azuelos, Neutron lifetime measurement with a helium-filled time projection chamber, *Nucl. Phys. A* **503**, 473 (1989).
- [32] K. Hirota, G. Ichikawa, S. Ieki, T. Ino, Y. Iwashita, M. Kitaguchi, R. Kitahara, J. Koga, K. Mishima, T. Mogi, K. Morikawa, A. Morishita, N. Nagakura, H. Oide, H. Okabe, H. Otono, Y. Seki, D. Sekiba, T. Shima, H. M. Shimizu, N. Sumi, H. Sumino, T. Tomita, H. Uehara, T. Yamada, S. Yamashita, K. Yano, M. Yokohashi, and T. Yoshioka, Neutron lifetime measurement with pulsed cold neutrons, *Prog. Theor. Exp. Phys.* **2020**, 123C02 (2020).
- [33] K. Mishima, T. Ino, K. Sakai, T. Shinohara, K. Hirota, K. Ikeda, H. Sato, Y. Otake, H. Ohmori, S. Muto, *et al.*, Design of neutron beamline for fundamental physics at J-PARC BL05, *Nucl. Instrum. Methods Phys. Res., Sect. A* **600**, 342 (2009).
- [34] K. Nakajima, Y. Kawakita, S. Itoh, J. Abe, K. Aizawa, H. Aoki, H. Endo, M. Fujita, K. Funakoshi, W. Gong, *et al.*, Materials and Life Science Experimental Facility (MLF) at the Japan Proton Accelerator Research Complex II: Neutron Scattering Instruments, *Quantum Beam Sci.* **1**, 9 (2017).
- [35] K. Taketani, T. Ebisawa, M. Hino, K. Hirota, T. Ino, M. Kitaguchi, K. Mishima, S. Muto, H. Oide, T. Oku, *et al.*, A high S/N ratio spin flip chopper system for a pulsed neutron source, *Nucl. Instrum. Methods Phys. Res., Sect. A* **634**, S134 (2011).
- [36] G. Ichikawa, Y. Fuwa, T. Hasegawa, M. Hino, K. Hirota, T. Ino, Y. Iwashita, M. Kitaguchi, J. Koga, S. Matsuzaki, *et al.*, Neutron lifetime experiment with pulsed cold neutrons at J-PARC, in *Proceedings of Particles and Nuclei International Conference 2021 — PoS(PANIC2021)*, Vol. 380 (2022) p. 457.
- [37] K. Mishima, G. Ichikawa, Y. Fuwa, T. Hasegawa, M. Hino, R. Hosokawa, T. Ino, Y. Iwashita, M. Kitaguchi, S. Matsuzaki, *et al.*, Performance of the Fully Equipped Spin Flip Chopper for the Neutron Lifetime Experiment at J-PARC, *Prog. Theor. Exp. Phys.* **2024**, 093G01 (2024).
- [38] Y. Arimoto, N. Higashi, Y. Igarashi, Y. Iwashita, T. Ino, R. Katayama, M. Kitaguchi, R. Kitahara, H. Matsumura, K. Mishima, *et al.*, Development of time projection chamber for precise neutron lifetime measurement using pulsed cold neutron beams, *Nucl. Instrum. Methods Phys. Res., Sect. A* **799**, 187 (2015).
- [39] J. Koga, S. Ieki, A. Kimura, M. Kitaguchi, R. Kitahara, K. Mishima, N. Nagakura, T. Okudaira, H. Otono, H. Shimizu, *et al.*, Measurement of gamma rays from ${}^6\text{LiF}$ tile as an inner wall of a neutron-decay detector, *J. Instrum.* **16**, P02001 (2021).
- [40] J. Allison, K. Amako, J. Apostolakis, P. Arce, M. Asai, T. Aso, E. Bagli, A. Bagulya, S. Banerjee, G. Barrand, *et al.*, Recent developments in Geant4, *Nucl. Instrum. Methods Phys. Res., Sect. A* **835**, 186 (2016).

- [41] H. Sumino, K. Nagao, and K. Notsu, Highly sensitive and precise measurement of helium isotopes using a mass spectrometer with double collector system, *J. Mass Spectrom. Soc. Jpn.* **49**, 61 (2001).
- [42] K. Mishima, H. Sumino, T. Yamada, S. Ieki, N. Nagakura, H. Otono, and H. Oide, Accurate determination of the absolute $^3\text{He}/^4\text{He}$ ratio of a synthesized helium standard gas (helium standard of Japan, HESJ): toward revision of the atmospheric $^3\text{He}/^4\text{He}$ ratio, *Geochem. Geophys. Geosyst.* **19**, 3995 (2018).
- [43] R. Kitahara, K. Hirota, S. Ieki, T. Ino, Y. Iwashita, M. Kitaguchi, J. Koga, K. Mishima, A. Morishita, N. Nagakura, *et al.*, Improved accuracy in the determination of the thermal cross section of $^{14}\text{N}(n, p)^{14}\text{C}$ for neutron lifetime measurement, *Prog. Theor. Exp. Phys.* **2019**, 093C01 (2019).
- [44] T. Mogi, T. Hasegawa, K. Hirota, G. Ichikawa, S. Ieki, T. Ino, Y. Iwashita, S. Kajiwara, Y. Kato, M. Kitaguchi, *et al.*, Improvement of systematic uncertainties for the neutron lifetime experiment at J-PARC, in *Proceedings of Particles and Nuclei International Conference 2021 — PoS(PANIC2021)*, Vol. 380 (2022) p. 458.
- [45] I. Katsioulas, P. Knights, and K. Nikolopoulos, Ionisation quenching factors from w-values in pure gases for rare event searches, *Astropart. Phys.* **141**, 102707 (2022).
- [46] J. F. Ziegler, M. D. Ziegler, and J. P. Biersack, SRIM—The stopping and range of ions in matter (2010), *Nucl. Instrum. Methods Phys. Res., Sect. B* **268**, 1818 (2010).
- [47] Tatsuhiko Sato and Yosuke Iwamoto and Shintaro Hashimoto and Tatsuhiko Ogawa and Takuya Furuta and Shin-ichiro Abe and Takeshi Kai and Pi-En Tsai and Norihiro Matsuda and Hiroshi Iwase and Nobuhiro Shigyo and Lembit Sihver and Koji Niita, Features of Particle and Heavy Ion Transport code System (PHITS) version 3.02, *J. Nucl. Sci. Technol.* **55**, 684 (2018).
- [48] S. F. Mughabghab, *Atlas of Neutron Resonances: Resonance Parameters and Thermal Cross Sections. Z= 1-100* (Elsevier, Amsterdam, 2006).
- [49] J. Als-Nielsen and O. Dietrich, Slow Neutron Cross Sections for ^3He , B, and Au, *Phys. Rev.* **133**, B925 (1964).
- [50] V. P. Alfimenkov, G. G. Akopyan, J. Wierzbicki, A. M. Govorov, L. B. Pikel'ner, and E. Sharapov, Neutron scattering lengths for ^3He , *Yad. Fiz.* **25**, 1145 (1977), [*Sov. J. Nucl. Phys.* **25**, 1145 (1977) (English translation)].
- [51] H. Otono, LiNA—Lifetime of neutron apparatus with time projection chamber and solenoid coil, *Nucl. Instrum. Methods Phys. Res., Sect. A* **845**, 278 (2017).
- [52] N. Sumi, G. Ichikawa, K. Mishima, Y. Makida, M. Kitaguchi, S. Makise, S. Matsuzaki, T. Nagano, M. Tanida, H. Uehara, *et al.*, The LiNA experiment: Development of multi-layered time projection chamber, *Nucl. Instrum. Methods Phys. Res., Sect. A* **1045**, 167586 (2023).